Dynamic Modelling of a Heat Exchanger Network for a Dairy Plant

Dynamic Modelling of a Heat Exchanger Network for a Dairy Plant

Riccardo Casadei[1], Marco Lorenzini[2], Daniele Fattini[1], Paolo Valdiserri[3]

[1] CoStell Srl, Via Dragoni, 59 I-47122 Forlì, I
[2] Università di Bologna, DIN - Dipartimento di Ingegneria Industriale, Via Fontanelle 40, I-47121 Forlì, I
3 Università di Bologna, DIN - Dipartimento di Ingegneria Industriale, Viale Risorgimento 2, I-40136 Bologna, I

E-mail: marco.lorenzini@unibo.it

Abstract. In co- and trigeneration plants with internal combustion engines, waste heat from their cooling system can be fed to a heat exchanger network for office heating, hot water production, or used in industrial processes. At the same time, care must be exerted not to cool the return fluid below a threshold, in order to avoid piston seizure. In this work, the heat exchanger network is that of a gas-engine trigeneration system for a large dairy plant in Rome. Since its daily and weekly production schedule is subject to several changes, temperature control must be both precise and efficient. A thermal-hydraulic, dynamic (i.e. time-dependent) model of the heat exchanger network was developed in Matlab/Simulink, to obtain the instantaneous pressure, mass flowrate and temperature of the fluids along the network. The approach is mixed, a lumped-parameter description of the hydraulic and thermal networ, and finite volumes for the heat exchangers. The model has been verified and validated with experimental, steady-state data from the dairy plant and the results found satisfactory.

1. Introduction

Many industrial facilities simultaneously require heat and power, which can be efficiently supplied by cogeneration and trigeneration systems [1, 2]. Gas turbines and internal combustion engines represent the most widespread means of electric power production in the medium range (1 to 10 MW): heat and, in the case of trigeneration, cold are obtained using the thermal energy of the flue gases (high temperature) and cooling fluids (low temperature). Gas engines coupled with an electric generator, also known as Genset, working according to a supercharged Miller cycle, have high power outputs, with about 28% of the primary energy transferred to the flue gas, and some $21-23\%$ to the cooling loop for the engine (lube oil, intercooler and jacket). Flue gases and cooling loop supply thermal energy at two different temperature levels, the former somewhat higher than the latter, which cannot be employed for steam production, but can find other uses, e.g. for space heating or absorption refrigeration. One problem which may arise when exploiting the colder fluid is that the return temperature may be too low. As a consequence, it is crucial to accurately control the total power transferred in order not to have too low a temperature of the return water, lest seizure of the pistons might occur, especially in cases when several users are connected to the network and their demands change abruptly and often in

time. This is the case for dairies, in which cogeneration has been suggested and implemented for a long time, [3, 4]. Since the daily and weekly production schedule of a large dairy is subject to several sudden changes, control must be both precise and efficient. Simulation tools can therefore be useful to investigate the network's response to changes in the load from the users and in operating parameters; moreover, they can be employed to detect potentially dangerous operating conditions, which might hinder smooth plant operation. In this paper, the thermal-hydraulic model of the heat exchanger network which uses the low-temperature waste heat from the Genset is detailed. The model is developed in Matlab/Simulink using a lumped-parameter approach for the hydraulic part and a mixed lumped-parameter/finite volume formulation in the thermal part. Verification and validation of the model have been carried out using steady-state experimental data, since the heat exchanger network is not yet fully operative.

2. Thermal-hydraulic model

The thermal-hydraulic model aims at predicting the behaviour of the heat exchanger network in terms of energy fluxes and mass flowrate and temperature of the working fluids at any given time, depending on the control parameters and the boundary conditions. The latter are the input mass flowrate and temperature on the cold side of the heat exchangers and the same quantities at the hydraulic separator, which connects the cooling loop of the Genset to the heat exchanger network. Control parameters are the valve openings and the rotational speed of the pump, which is steered by an inverter. The hydraulic and thermal models are treated separately: knowledge of the pressure distribution allows computation of the mass flowrates in the various heat exchangers, with the exchanged power determined by the thermal model. The model was developed with a mixed analytical and experimental approach, as detailed in the following and implemented through Simulink. A sketch of the network is shown in Fig. 1.

It can be clearly recognised that the network consists of three subsystems, $c1$, $c2$ and $c3$, each with several heat exchangers in parallel. The network receives the hot cooling fluid from the Genset through the hydraulic separator (far left in Fig. 1), whose pressure is the reference value for the network. Circuit $c1$ groups the plate heat exchanger used for room heating and two shell-and tube heat exchangers for the cleaning in place (CIP) of the milk tankers. All three devices are steered by pneumatic valves; also an end-line manual valve is present, to create a fixed-impedance circuit branch. The second subsystem, $c2$, groups three pasteurisers, each steered by a pneumatic valve and with a small fixed-speed pump that favours circulation in the last section of the network, $c3$, where eight plate heat exchangers serve as fluid pre-heaters for other CIP tasks. The hot fluid from the hydraulic separator is circulated to the head collector by a double centrifugal pump with asynchronous motor controlled by an inverter; the cold fluid coming from the three subsections mixes in the cold-end collector and reaches the hydraulic separator again. The temperature of the hot cooling fluid is set at $T_{HF} = 90\,°C$, so, neglecting heat losses along the piping, the thermal power through each heat exchanger depends solely on the mass flowrate through it, which is determined both by the rotational speed of the pump (overall mass circulated) and by the flow characteristic of each control valve (flowrate through each heat exchanger).

3. The hydraulic model

The hydraulic model is developed following a lumped-parameter approach, [5, 6], based on the assumptions below:

- The working fluid (water) is considered incompressible,no phase change occurs.
- Fluid density is constant owing to its modest variation in the temperature range considered.
- Pressure variations propagate at infinite speed, since the ducts are comparatively short.
- Ducts are rigid and non deformable.

- Capacitive effects in the expansion tanks are neglected.

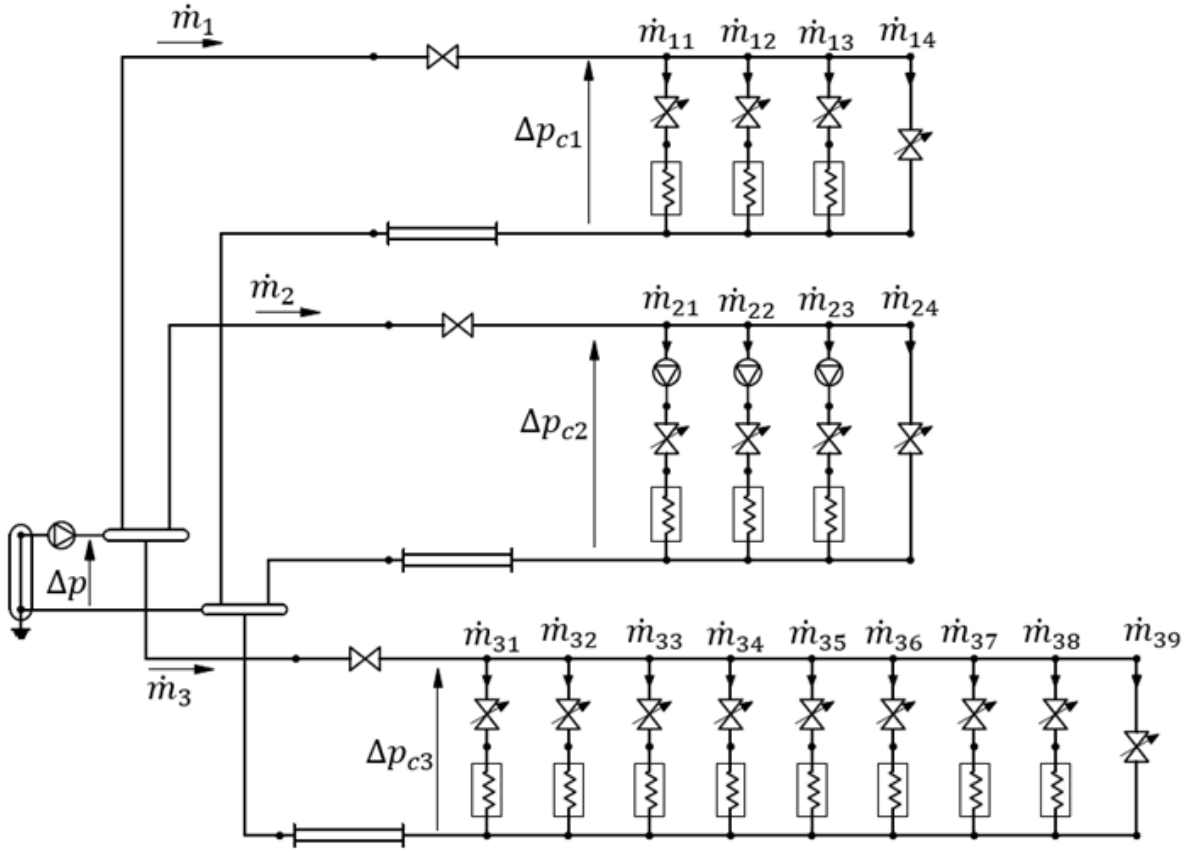

Figure 1. Sketch of the heat exchanger network.

The main circulation pump generates a pressure difference Δp between the hot and cold collectors which is a function of the mass flowrate $\dot{m}$ through it and of the speed of revolution, which is expressed as a percentage of its maximum value, $\%n_{max}$. The mass flowrate is dictated by the overall hydraulic characteristic of the circuit, whereas the speed of revolution is determined by the pump's control system. As can be seen from the sketch, Fig. 1, the total mass flowrate is split into three streams, $\dot{m}_i$, which are further divided according to the number of branches each of the three subsystem has. The flowrate through the j-th branch of the i-th subsystem is $\dot{m}_{ij}$. To estimate the instantaneous flowrate through each branch, which contains one pump, one one valve and one heat exchanger at most, see Fig. 2, a momentum balance must be written. Accounting for the inertial contribution due to the fluid in the piping and heat exchanger, the momentum balance yields

$$\frac{V_{hx} + L \cdot S}{S^2} \frac{d\dot{m}}{d\tau} = \Delta p + \Delta p_p - \Delta p_v - \Delta p_{hx} \tag{1}$$

where V_{Hx} is the volume of the fluid in the heat exchanger, L is the length of the piping, S its cross-sectional area, and the subscripts p, v and hx refer to the pump, valve and heat exchanger respectively.

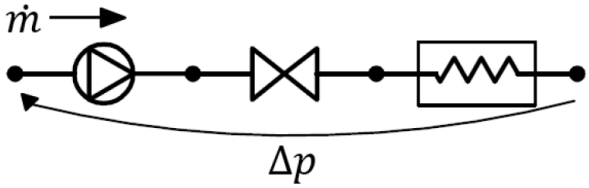

Figure 2. Single branch of the heat exchanger network.

Since the pump operates at a fixed speed, its pressure drop can be described quite accurately as the difference between the rated head, H_0 and the product of a loss coefficient times the square of the mass flowrate through the pump:

$$\Delta p_p = H_0 - R_p \cdot \dot{m}^2 \tag{2}$$

The pressure drop associated with the valves can be expressed, after some rearranging, as a function of the mass flowrate times a constant depending on the valve opening a, of its flow coefficient at full opening, $K_{v,a}$, of the fluid density at a reference temperature, ρ_0 and at the operating temperature, ρ

$$\Delta p_v = \frac{1}{\rho \cdot \rho_0 \cdot K_{v,a}^2} \left(\frac{\dot{m}}{a^b}\right)^2 = \left(\frac{R_v}{a^{2b}}\right) \cdot \dot{m}^2 \tag{3}$$

This form applies to both equal percentage and linear opening valves, for the latter $b = 1$, the two types mounted in the network.

3.1. Pressure drop in the heat exchangers

Pressure drop in the heat exchangers can be cast into the same form, regardless of their type, i.e.

$$\Delta p_{hx} = R_1 \cdot \mu^{-B} \cdot \Phi_s^{-1} \dot{m}^{2+B} + R_2 \cdot \Phi_s^{-1} \dot{m}^2 + R_3 \cdot \dot{m}^2 \tag{4}$$

The values of R_i depend on the type of heat exchanger (in this case plate or shell-and-tube) of its geometry and of the fluid density, and are therefore constants; $\Phi_S = (\mu/\mu_w)^{0.17}$ is the ratio of the fluid viscosity at the bulk temperature, μ, to that at the wall temperature, μ_w and B is a coefficient which depends on the type of heat exchanger, and for shell-and-tube realizations, on the side (i.e. shell or tube) through which the fluid flows. The expressions of R_i for each type of heat exchanger are omitted for the sake of brevity, the interested reader is referred to [7]; what is important, is that their values do not change during operation of the network. They can therefore be determined by tests on the heat exchangers at three different values of the mass flowrate, provided that both the viscosity ratio and B are known. The viscosity ratio is obtained by temperature measurements at the inlets and outlets of the heat exchanger, whereas for plate heat exchangers and for the tube side of shell-and-tube devices $B \approx -1$, [8], whilst for the shell side B is computed with Kern's method, [7], and is -0.19. Substituting Eqs. (2)-(4) into Eq. (1) relates the mass flowrate change to the pressure difference and to the mass flowrate, yet inertial effects only account for the fluid in the pipe length from pump inlet to heat exchanger outlet. With reference to Fig. 1, there is also a contribution by the length of pipe from the main pump to the single branch, which must be accounted for to correctly predict the mass flowrates rates of change in the whole network. If $'i'$ is the index that refers to the subnet and $'j'$ to the branch in the subnet (from one to a maximum of nine branches are present in each of the three subnets),

the governing equation has the form

$$\frac{d\dot{m}_{ij}}{d\tau} = \frac{\Delta p(\dot{m}, \%n) - R_i \dot{m}_i^2 + H_{0,ij}}{3\frac{4L_i}{\pi d_i^2} + \frac{V_{hx,ij}+L_{ij}\cdot S_{ij}}{S_{ij}^2}} - \\ - \frac{\left[R_{p,ij} + \left(\frac{R_{v,ij}}{a^{2b}}\right) + R_{1,ij}\mu_{ij}^{-B}\Phi_{s,ij}^{-1}\dot{m}_{ij}^{B} + R_{2,ij}\mu_{ij}^{-B}\Phi_{s,ij}^{-1} + R_{3,ij}\right]\dot{m}_{ij}^2}{3\frac{4L_i}{\pi d_i^2} + \frac{V_{hx,ij}+L_{ij}\cdot S_{ij}}{S_{ij}^2}} \tag{5}$$

The system of equations thus obtained is solved via Simulink. With reference to Fig. 3, the inlet fluid temperatures at each time step allow the current viscosity to be computed using a lookup table, together with the correction coefficients Φ_s for each branch; heat losses along the piping are neglected (as they are normally well below $1\,K$, [8], therefore these are the same as the end-line values. The remaining inputs are the mass flowrates at the current time step, which are known as a result of the previous integration loop, the opening of the valves, and the the percentage of the maximum speed of revolution of the pump. These, together with the total mass flowrate, allow calculation of the current pump head, $\Delta p(\dot{m}, \%n)$. The new time derivative of the mass flowrate are thus computed and, by integration, the mass flowrates, both total and for each branch of the network, are obtained.

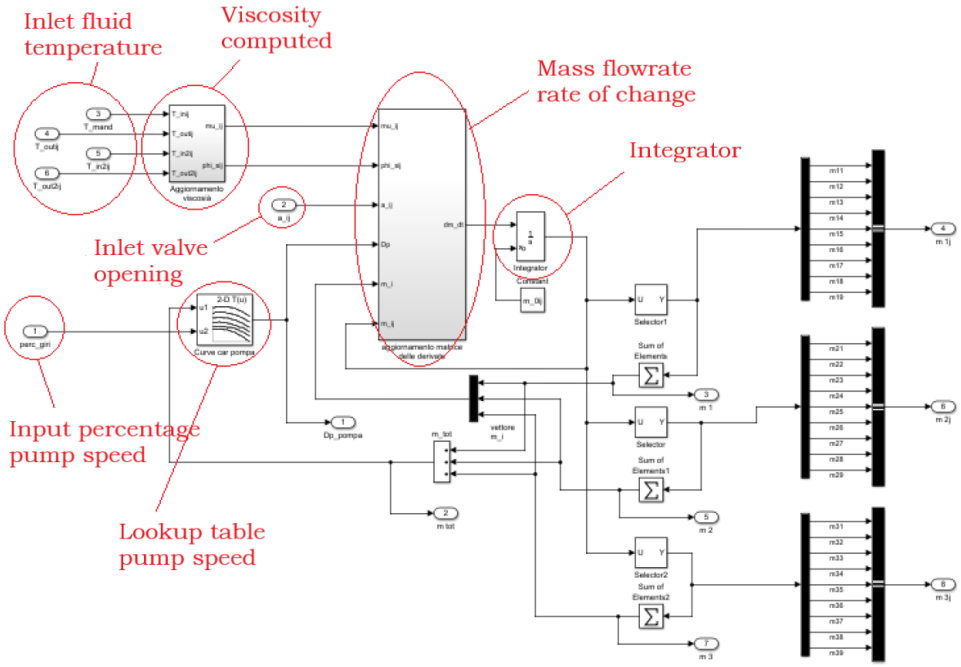

Figure 3. Simulink subsystem to calculate the instantaneous flowrate.

4. Thermal model

The thermal model receives the mass flowrates from the hydraulic model and the input temperatures and yields the outlet temperatures and computed heat fluxes in all the heat exchangers in the network. The hot fluid from the hydraulic separator heats the cold fluid in the heat exchangers which are working at a given time, and is then collected downstream

before entering the separator again at its cold end. Concerning the cold fluids in the heat exchangers, their inlet temperatures are constant during operation, whilst their flowrates are either constant, if they are fed to the device using an 'on-off' logic, or vary proportional to the flowrate on the hot side of the heat exchanger. The maximum thermal power available in the hydraulic separator is $\dot{Q}_{max} = 750\,kW$, but can be lower depending on the working conditions of the Genset, and can drop to zero if three-way valve bypasses the separator, in case seizure might otherwise occur. Three assumptions are made in setting up the model:

- Thermal losses along the lines and in the heat exchangers are altogether neglected.
- The fluid is incompressible, has constant thermal capacity and is not subject to phase change.
- Temperature variations travel along the ducts at the same velocity as the bulk fluid.

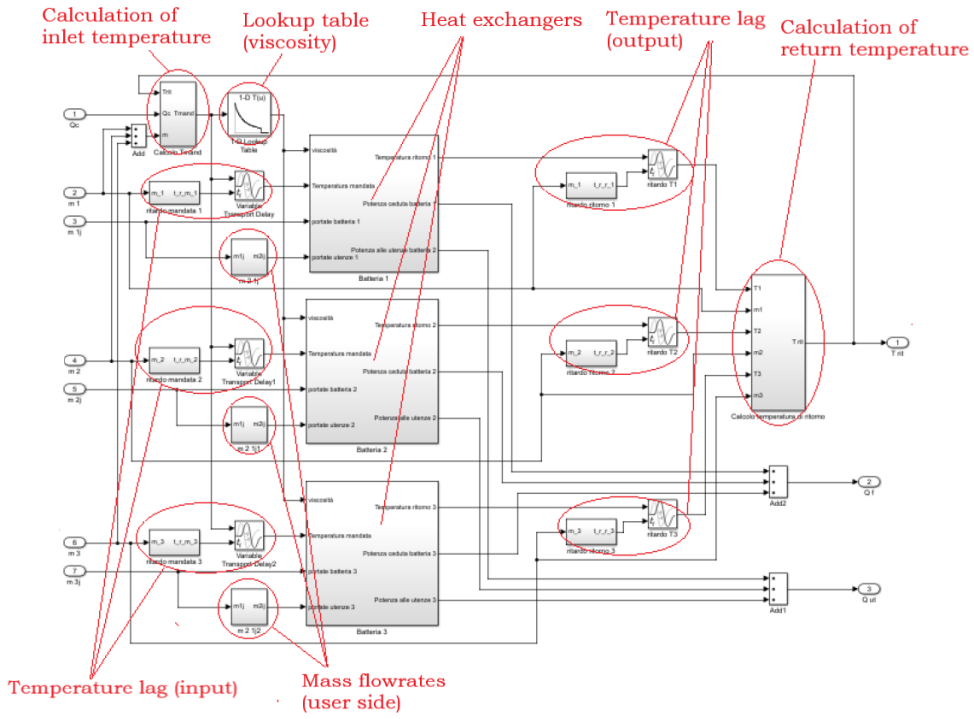

Figure 4. Simulink subsystem for the heat exchangers.

Concerning the last assumption, a sudden change in the heat transfer at a given heat exchanger causes a change in the outlet temperature of the hot fluid, which will travel along the pipe with a certain lag. In fact the time τ_d needed to cover the length of the duct is

$$\tau_d = \frac{L \cdot S \cdot \rho}{\dot{m}} \tag{6}$$

Contrary to what happened for the hydraulic model, the thermal model is influenced by the plant upstream of the hydraulic separator, as the available thermal power depends on the operating conditions of the Genset. Nonetheless, this can be easily incorporated into the model as a time-dependent thermal source $\dot{Q}(\tau)$ which increases the return temperature of the hot fluid of the heat exchanger network. The outlet temperature of the hot fluid, $T_{o,ij}$,changes for each

branch in a subnet, and the subnet outlet temperature is computed as the weighted average of the outlet temperatures from the heat exchangers and end-line, so that

$$T_{o,i} = \frac{1}{\dot{m}_i} \sum_{j=1}^{n} \dot{m}_{ij} \cdot T_{o,ij} \tag{7}$$

The temperature lag is considered only in the input and return pipes to the subnet, as these stretches are much longer than the piping in the branches of the subnets. Thus, a change in the power input from the cooling loop of the Genset will cause a change in the inlet temperature at the subnet after a time $\tau_{d,e}$ whilst a change in the return temperature will reach the downstream collector after a time $\tau_{d,r}$. The working principle of the thermal model can be illustrated with reference to Fig. 4. At each time step the mass flowrates (both of the hot fluid and of the cold fluids from the users), the instantaneous heat flux from the cooling loop and the return temperature of the hot fluid are the inputs which allow to calculate the instantaneous temperature; the time lag is also computed by means of a specific Simulink block called 'variable transport delay', and thus the input temperature to the heat exchangers in the branches of the sub-network can be determined. The outlet temperatures and exchanged thermal power in the heat exchangers are computed for the next time step, and the resulting temperature, Eq. (7), at the outlet of each sub-network is obtained, as is the time lag of the return temperature, hence the exit temperature from the downstream collector is obtained, which is the input temperature for the hydraulic separator, and closes the computation loop.

4.1. Modelling of the heat exchangers

The number of heat exchangers actually working at a given time is dependent on the thermal demands of the end-users. It is therefore likely that the inlets of some heat exchangers are shut off, and then re-opened at a later time. If the shut-off time is long enough, though, the fluid within the heat exchangers cools and, when operation resumes, it is injected in the network, which may cause a so-called 'cold wave', i.e. a significant decrease in the bulk temperature of the fluid, which propagates along the ducts, and can be detrimental for the Genset, as the jackets would be cooled below a threshold temperature, thus causing seizure of the engine's pistons. It has been verified that cold waves can occur in the actual network, and this poses a modelling issue which make the lumped-parameter approach unsatisfactory. In order to be able to capture, and thus avoid, the occurrence of cold waves, the heat exchangers of both types (single pass, plate and single-pass shell-and-tube) have been modelled using a finite-volume approach, which allows consideration of the thermal inertia of the heat exchanger itself and of the fluid masses within. In the following, for brevity's sake, the procedure is detailed for the plate heat exchanger only; it is similar, for the shell-and tube type, although slightly more involved, owing to the different path of the fluid on the shell side. Discretising the the energy balance equations, [7, 9], the time derivatives of the temperature for the cold (subscript c) and hot (subscript h) fluids and for the channel wall (subscript w) become, for the i-th inner element

$$\frac{dT_w}{d\tau} = \frac{\Delta\dot{Q}_{h(i)} - \Delta\dot{Q}_{c(i)}}{\rho \cdot c \cdot \Delta V} \tag{8}$$

$$\frac{dT_{h(i)}}{d\tau} = \frac{\dot{m}_h \cdot c_{p,h}\Big(T_{h(i-1)} - T_{h(i)}\Big) - \Delta\dot{Q}_{h(i)}}{\rho_h \cdot c_{p,h} \cdot \Delta V_h} \tag{9}$$

$$\frac{dT_{c(i)}}{d\tau} = \frac{\dot{m}_c \cdot c_{p,c}\Big(T_{c(i\pm1)} - T_{c(i)}\Big) + \Delta\dot{Q}_{c(i)}}{\rho_c \cdot c_{p,c} \cdot \Delta V_c} \tag{10}$$

In Eq. (10) the $\pm$ is for counterflow and co-flow arrangements respectively. The same expressions are valid for the shell-and-tube heat exchangers. In Eqs. (8)-(10) two heat fluxes appear, whose expressions are

$$\Delta\dot{Q}_{h(i)} = U_h \Delta A_p \Big(T_{h(i)} - T_{w(i)} \Big) \tag{11}$$

$$\Delta\dot{Q}_{c(i)} = U_c \Delta A_p \Big(T_{w(i)} - T_{c(i)} \Big) \tag{12}$$

where ΔA_p is the heat transfer area between fluid and channel wall and U is the overall heat transfer coefficients between either fluid and the wall, which is of thickness t and thermal conductivity κ_w

$$U = \frac{1}{\frac{1}{h} + \frac{t}{2 \cdot \kappa_w}} \tag{13}$$

where h is the heat transfer coefficient for the fluid involved. The latter quantity can be obtained from the correlations yielding the Nusselt number for plate heat exchangers, which are also dependent on the chevron angle, β of the plates, [7]. It can be shown that

$$h = \frac{\kappa}{D_h} \cdot C_h(\beta) \cdot Re^n \cdot Pr^{1/3} \Phi_s \tag{14}$$

This would make computation of the convective heat transfer coefficient lengthy and impractical for the simulation; a lookup table was therefore devised starting from the fit of the group $C_h(\beta) \cdot Re^n$:

$$C_h(\beta) \cdot Re^n = F \cdot Re^E \tag{15}$$

with E and F determined through fitting and are constant over the whole range of Reynolds numbers of interest, whereas $C_h(\beta)$ and n are only piecewise constant. Using Eq. (15), the expression for h becomes

$$h = H(E, F) \cdot \mu^{1/3-E} \cdot \Phi_s \cdot \dot{m}^E \tag{16}$$

For the shell-and-tube configuration, the shell-side overall heat transfer coefficient is obtained by a similar procedure, but must be corrected before being used in the discretised model in order to account for the mixing of the various streams around the tubes at the shell side. The algorithm requires the initial temperature distribution at the nodes and the inlet temperature and flowrates of the hot and cold fluid and yields the exchanged thermal power and the outlet fluid temperatures over time.

5. Verification and validation

The model has been validated for the hydraulic part by carrying out a steady-state measurement of the pressure head of the main twin pump for isothermal flow of water through the network, from 50% to full speed. The measured pressure head ranged from $0.59\,bar$ to $2.36\,bar$, and the model yielded values of $0.61\,bar$ and 2.38, with a maximum discrepancy over the whole range of experimental data below $\pm 3.3\%$, which was deemed quite satisfactory.

The thermal model was first verified by checking that it could replicate the $\varepsilon - NTU$ plot for the plate and shell-and-tube heat exchangers correctly. The results are shown for two different values of the capacity ratio C_r in Figs. 5 and 6.

For the shell-and-tube arrangement, one value of the effectiveness,ε, for $C_r = 0.667$ and $C_r = 0.350$ was known from the manufacturer and is plotted in Figs. 7 and 8, together with the effectiveness-NTU curves for a cross-flow realisation with complete mixing on the shell-side. The results of the model, both with the uncorrected and the corrected overall heat transfer coefficient, are also plotted. The value of the correction factor was obtained for $C_r = 0.667$. Finally, one

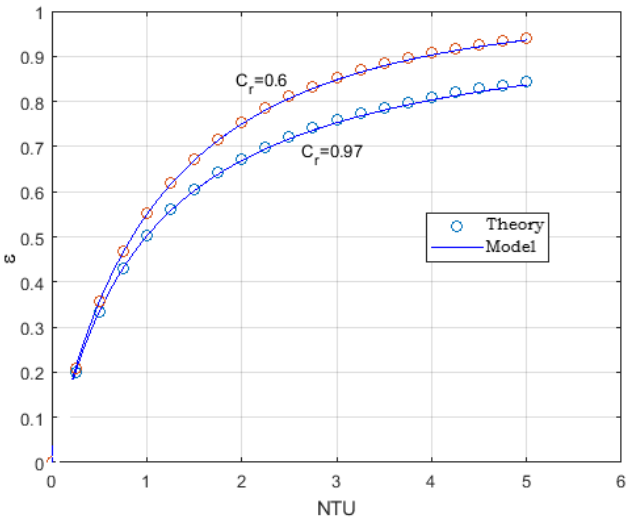

Figure 5. Comparison of $\varepsilon - NTU$ curves: plate heat exchanger in counterflow.

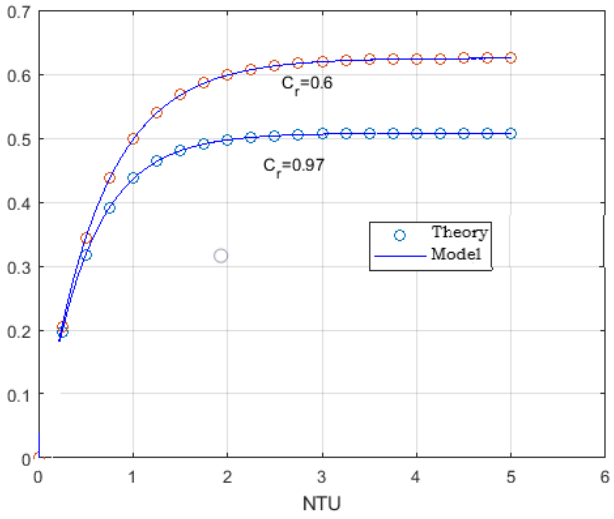

Figure 6. Comparison of $\varepsilon - NTU$ curves: plate heat exchanger in co-flow.

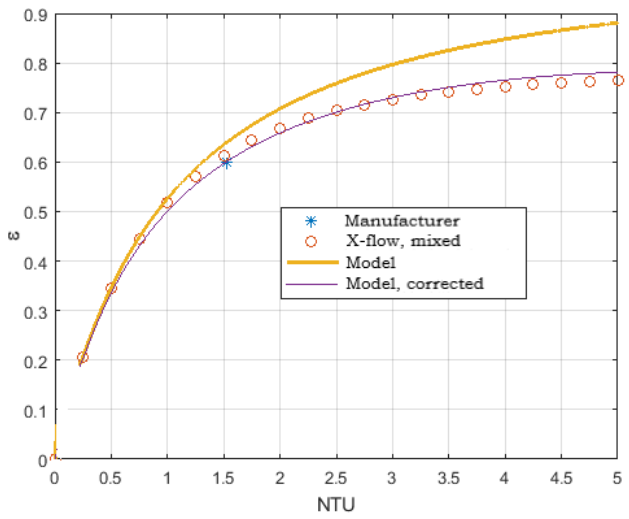

Figure 7. Shell-and-tube heat exchanger with $C_f = 0.667$.

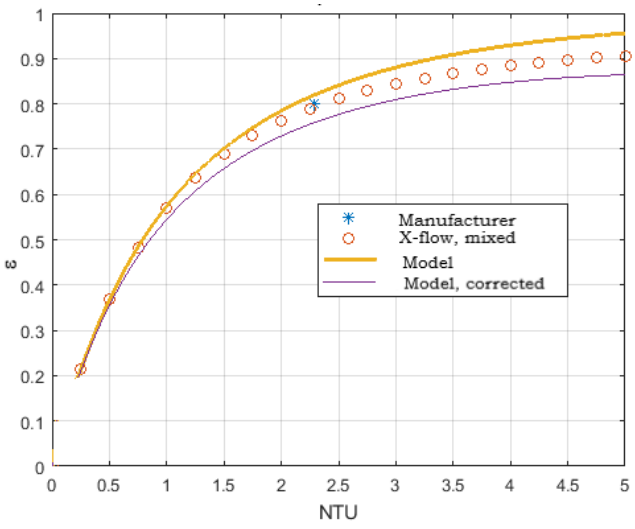

Figure 8. Shell-and-tube heat exchanger with $C_f = 0.350$.

test was made comparing the results from the model to those obtained under steady conditions in one heat exchanger, during a CIP operation. The mass flowrates on the hot and cold side were $\dot{m}_h = 8.62\, kg \cdot s^{-1}$ and $\dot{m}_c = 6.47\, kg \cdot s^{-1}$ respectively, and the inlet temperatures for the hot and cold fluids $T_{h,in} = 90\,°C$ and $T_{c,in} = 55\,°C$. The measured heat flux amounted to $\dot{Q} = 539\, kW$, against a predicted value of $\dot{Q} = 542.8\, kW$; the measured outlet temperatures were $T_{h,ex} = 75\,°C$ and $T_{c,ex} = 75\,°C$, whereas the model predicted $T_{h,ex} = 74.9\,°C$ and $T_{c,ex} = 75.1\,°C$, thus showing an excellent agreement with the experimental data. The model can also be extended to allow the determination of the exergy fluxes involved and, thus, a second-law analysis of the performance. The methodology adopted, moreover, can be applied to any similar network of heat exchangers.

At the time of writing the heat exchanger network is not yet fully operative, therefore no

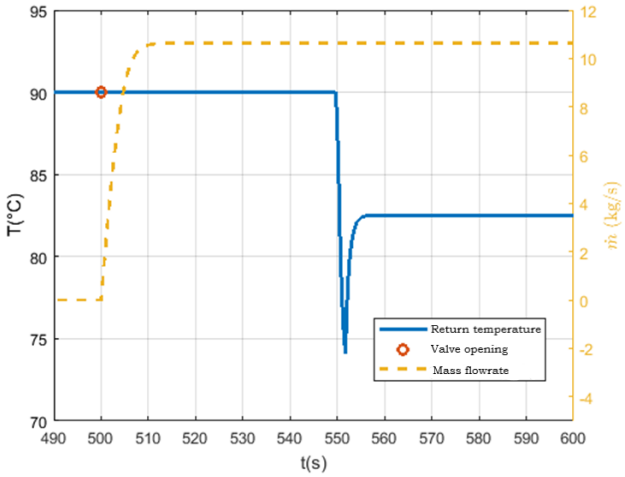

Figure 9. Flowrate and temperature changes due to one heat exchanger starting to operate.

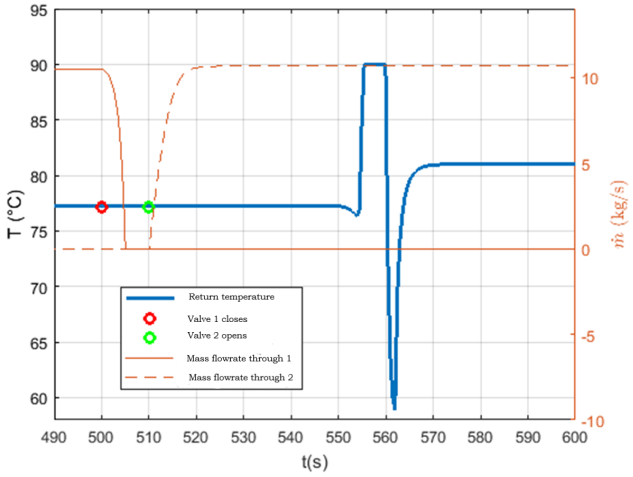

Figure 10. Flowrate and temperature changes due to one heat exchanger shutting off and another starting shortly after.

dynamic validation is possible. Yet, once this is carried out, the model can be used to determine the evolution of the return temperature of the hot fluid, so as to avoid piston seizure, and to investigate the energy performance of the network: two examples are given in Fig. 9 for the case of the sudden opening of one heat exchanger's valve and in Fig. 10 for one heat exchanger being shut off and another one being open after a short delay. Changes in both mass flowrates and temperatures can be appreciated, as well as the delay in the latter, owing to the length of the piping.

6. Conclusions

In this paper a dynamic model describing the thermal-hydraulic behaviour of a heat exchanger network serving a dairy industry has been described and verified against steady-state measurements. The network can be used both to prevent cold waves issuing during operations, which may damage the Genset, and to evaluate the amount of waste heat recovered depending on the operation modes.

References

[1] Murugan S and Horák B 2016 *Renewable and Sustainable Energy Reviews* **60** 1032–1051
[2] Raj N T, Iniyan S and Goic R 2011 *Renewable and Sustainable Energy Reviews* **15** 3640–3648
[3] Van Huffel P L 1984 *Energy Technology: Proceedings of the Energy Technology Conference* pp 673–685
[4] Correia V H L, Abreu R P D and Carvalho M 2021 *Journal of Cleaner Production* **314**
[5] Lucchi M, Lorenzini M and Valdiserri P 2017 *Journal of Physics: Conference Series* vol 796
[6] Lucchi M and Lorenzini M 2019 *Applied Thermal Engineering* **147** 438–449
[7] Kakaç S and Liu H 1998 *Heat Exchangers: Selection, Rating and Thermal Design* (Boca Raton: CRC Press)
[8] Serth R W and Lestina T G 2014 *Process Heat Transfer: Principles, Application and Rules of Thumb* (New York: Academic Press)
[9] Nellis G and Klein S 2009 *Heat Transfer* (Cambridge: Cambridge University Press)